Front. Phys., 2012, 7(3): 353–359
DOI 10.1007/s11467-011-0209-9

RESEARCH ARTICLE

First principles study on magnetic and electronic properties with rare-earth atoms doped SWCNTs

Shun-li Yue, Hong Zhang†

College of Physical Science and Technology, Sichuan University, Chengdu 610065, China

E-mail: †hongzhang@scu.edu.cn

Received July 13, 2011; accepted August 17, 2011

The adsorptions of rare-earth (RE) atoms on (6, 0) and (8, 0) single-walled carbon nanotubes (SWCNTs) have been investigated by using the first-principles pseudopotential plane wave method within density functional theory (DFT). The binding energy, Mulliken charge, magnetic properties, band structure and DOS were calculated and analyzed. Most of RE atoms including Nd, Sm and Eu have a magnetic ground state with a significant magnetic moment. Some electrons transfer between RE-5d, 6s and C-2p orbitals. Owing to the curvature effect, the values of binding energy for RE atoms doped (6, 0) SWCNT are lower than those of the same atoms on (8, 0) SWCNT. The pictures of DOS show that hybridizations between RE-5d, 6s states and C-2p orbitals and between RE-4f and C-2p orbitals appear near the Fermi level. Results indicate that the properties of SWCNTs can be modified by the adsorptions of RE atoms.

Keywords DFT, RE atoms, single-walled carbon nanotubes (SWCNTs), doping

PACS numbers 81.05.Tp, 68.43.-h, 73.22.-f

1 Introduction

Since its discovery by Iiyima twenty years ago [1], carbon nanotubes (CNTs) have attracted a lot of attention from scientific community. This is because CNTs, especially SWCNTs (single-walled carbon nanotubes), have special geometries and unique properties [2, 3] that offer great application potentials, such as nanoelectronic devices [4], nanomagnets [5], hydrogen storage media [6], catalyst support [7] and so on. However, the properties of SWCNTs can be modified better by doping metal atoms. Upon the adsorptions of metal atoms, the electrical conductivity of SWCNTs changes remarkably [8]. As we know, hydrogen storage is an important issue [9–12]. Some metal atoms on SWCNTs can significantly enhance the hydrogen storage [13]. Meanwhile, the single-walled carbon nanotubes are produced by arc-discharge [14], laser ablation [15] or catalyst chemical vapor [16]. A common feature of these methods is the requirement of transition or rare-earth metal catalysts, so studies of the interaction between metal atoms and SWCNTs are badly needed.

Up to now, many researchers have widely investigated the adsorptions of alkali and transition metals (including a single atom, cluster and atomic wire) on the surface of SWCNTs or SWCNT bundles [17–25]. For instance, first-principles study has indicated that Li intercalated carbon nanotube ropes are promising candidate materials for anode in battery application [17]. The effect of doping transition metals (TMs) into single-walled carbon nanotubes was investigated [22]. It was found that the doping of Mn, Fe and Co make metallic (3, 3) SWCNT semi-metallic, while Ni doping leads it to a semiconductor. Durgun [20, 21] studied extensively the adsorptions of large numbers of individual atoms on the surface of (8, 0) and (6, 6) SWCNTs, and found that they have revealed the character and geometry of the bonding and the effect of adsorptions on the physical properties such as electronic and magnetic properties. However, to our knowledge there are a few reports on the interaction between rare-earth metals and SWCNTs and only Eu doped armchair carbon nanotubes [26] and Eu doped (8, 0) SWCNTs [27] were studied by density functional theory (DFT). The study of this interaction is essential in understanding the role that the rare-earth catalysts play in the process of SWCNTs growth [14]. And doping RE atoms can influence the magnetic properties of SWC-

NTs, which is the basis of nanomagnent. Furthermore, the hydrogen adsorption property of RE doped SWCNT is an interesting topic too, because the unpaired 4f electrons of RE (such as Eu) could serve as electron donors or acceptors to increase the binding energy for H_2 on SWCNT [28].

In this work, we study the interaction between SWCNTs and RE metals (La, Nd, Sm and Eu) by the ab inito calculations. The (6, 0) and (8, 0) SWCNTs were chosen here. Although they are both zigzag carbon nanotubes, they have different curvatures and conductivity. The (6, 0) SWCNT is a metal of 4.70 Å in diameter and the (8, 0) SWCNT is a common semiconductor with a diameter of 6.26 Å. The focus is placed on the effect on SWCNT by doping different RE atoms and the influence of the SWCNTs' curvature and conductivity. We present and discuss the structure, electronic and magnetic properties of RE doped SWCNTs.

2 Computational method

We used first-principles, pseudopotential, spin unrestricted density functional theory (DFT) as an implement in the DMol package [29, 30]. For the exchange and correlation terms, the generalized gradient approximation (GGA) with the Perdew, Burke and Ernzerhof (PBE) function was used. Previous work has confirmed that the DFT and GGA methods can be used to predict the structure of lanthanide complexes correctly [31–33]. DFT calculations with GGA describe the strong coulomb correction properly because GGA treats the nonlocality of exchange-correlation better than LDA [34–36]. Double numerical basis set with polarization function (DNP) was selected. The DFT semicore pseudopotential (DSPP) was performed for the relativistic effect, which replaces core electrons as a single effective potential [37].

In the present calculation, we applied a super hexagonal cell whose lattice constants (a and b) are 16 Å. In order to reduce the interaction of RE atoms in neighboring nanotube cells, two primitive cells were adopted in the axial direction for the zigzag (8, 0) and (6, 0) SWCNTs. The Brillouin zone integration was performed with the Monkhorst-pack scheme using $1\times1\times6$ k-points [38]. The global orbital cutoff was set to be 5.5 Å. In the meantime, the atomic positions in all of the computation models were fully relaxed until they had reached a convergence energy of 2×10^{-5} Ha (1 Ha = 27.2114 eV). The maximum force and the maximum stress were set to be 0.004 Ha/ Å and 0.005 Å, respectively. The charge and magnetic moment were obtained by Mulliken population analysis. For comparison, we used an identical simulation in all the computations.

3 Results and discussion

For most of single atoms doped outside of SWCNTs, the hollow site is more favorable than others. So in the present work we only discuss RE atoms doped in this site. First, we carried out the geometry optimization for the pure SWCNTs and RE doped SWCNTs, respectively. The original structure of RE atom doped (6, 0) and (8, 0) SWCNTs are shown in Fig. 1. Upon optimization the tube structures changed slightly. The C–C bonds of the C_6 rings near the RE atoms were elongated or shortened. And under the repulsion interaction, the distance from RE to CNT got a little longer. Based on the optimization structures, we calculated the average distance of RE to the six nearest carbon atoms, binding energy, magnetic moment and Mulliken charge. The binding energy was calculated by the following formula:

$$E_b = E_T[RE - SWCNT] - E_T[RE] - E_T[SWCNT] \quad (1)$$

where $E_T[RE - SWCNT]$ is the spin-polarized total energy for the optimized configuration of RE doped SWCNT, $E_T[RE]$ is the spin-polarized total energy of an RE atom (La, Nd, Sm or Eu) in the ground state, and $E_T[SWCNT]$ is the total energy of the pure optimized SWCNT. A summary of the results for the equilibrium structure was given in Table 1.

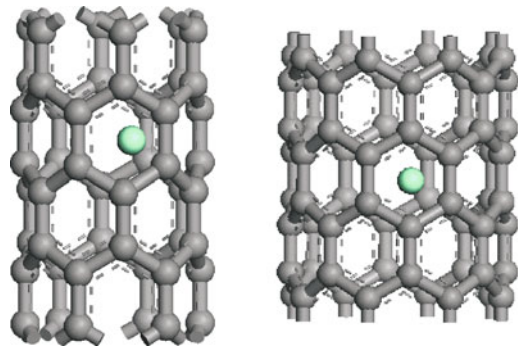

Fig. 1 The original structures of RE atom doped (6, 0) and (8, 0) SWCNTs, respectively.

As shown in Table 1, Nd is the most favorable dopant for (6, 0) SWCNT with a binding energy of −3.25 eV, which is lower than other cases. And the most favorable RE atom doped in (8, 0) carbon tube is La with a binding energy of −2.44 eV. It can be found from the obtained results that the value of binding energy ranges from −1.85 eV to −3.25 eV, thus the RE atoms are suitable to dope (8, 0) and (6, 0) SWCNTs. While the binding energy of an individual RE atom becomes lower for adsorption on the (6, 0) carbon nanotube in comparison with the (8, 0) carbon nanotube. This trend can be explained by the curvature effect, as shown in previous investigations [13, 39]. The average RE–C bond distances

Table 1 Summary of results for RE metal atoms adsorbed on the (6, 0) and (8, 0) carbon nanotubes. The average distance of adatom to six nearest carbon atoms, binding energy, magnetic moment on RE atoms, magnetic moment per supercell and Mulliken charge of RE atoms are listed here, respectively.

Model	$d_{\text{RE-C}}$/Å	E_{b} /eV	μ_{RE} /μ_{B}	$\mu_{\text{RE-CNT}}$ /μ_{B}	Charge/a. u.
La-(6, 0) SWCNT	2.70	–2.98	0.0	0.0	0.761
Nd-(6, 0) SWCNT	2.68	–3.25	–4.029	–3.967	0.597
Sm-(6, 0) SWCNT	2.69	–2.35	–6.215	–6.075	0.975
Eu-(6, 0) SWCNT	2.70	–2.18	7.234	7.182	0.963
La-(8, 0) SWCNT	2.69	–2.44	0.0	0.0	0.725
Nd-(8, 0) SWCNT	2.69	–2.42	–4.708	–3.988	0.546
Sm-(8, 0) SWCNT	2.68	–1.85	–6.273	–6.083	0.955
Eu-(8, 0) SWCNT	2.70	–1.67	7.327	7.299	0.930

range from 2.67 Å to 2.70 Å, which are larger than the distance of TM–C in transition metals doping cases [21]. The results of magnetic properties were also presented in Table 1. The magnetic moments of RE atoms (including Nd, Sm and Eu) are preserved after doping and the magnetic moment of doped SWCNT per supercell is slightly smaller than that of the adsorbed RE atom. Perhaps these systems can be used as potential materials for nanomagnets which have been applied in many fields [40]. This phenomenon can also be observed in TM doped carbon tubes [26] and RE doped C_{60} [41]. However, the adsorbed La has no magnetic moment ($0\,\mu_{\text{B}}$) and that of the free La atom is $2.220\,\mu_{\text{B}}$. The magnetic moments of Eu atom adsorbed onto (6, 0) and (8, 0) SWCNTs are 7.234 and $7.327\,\mu_{\text{B}}$, respectively. In the calculation of Eu doped (3, 3), (4, 4) and (6, 6) SWCNTs [22], the results are 7.162, 7.519 and $7.850\,\mu_{\text{B}}$, respectively. For (6, 0) and (8, 0) carbon tubes, the magnetic moments of Sm atom are 6.125 and $6.273\,\mu_{\text{B}}$, respectively. And in Lu's work [42], the magnetic moment of Sm doped C_{60} is $6.460\,\mu_{\text{B}}$. Our results for the magnetic moments agree closely with theirs.

For a further study, we calculated the electrons distribution on orbitals of RE and C atoms. Now we take La and Eu doped (8, 0) SWCNT as examples for analysis. The electronic configurations of La and Eu are [Xe] $4f^{0}5d^{1.752}6s^{1.248}$ and [Xe] $4f^{6.997}5d^{0.142}6s^{1.860}$ respectively before doping. They become [Xe] $4f^{0.066}5d^{1.768}6s^{0.312}$ and [Xe] $4f^{6.962}5d^{0.644}6s^{0.359}$ after the doping. And in the pure (8, 0) tube, the electronic configuration of C atom is [He] $2s^{1.262}2p^{2.671}$. Upon the doping of La and Eu, the electronic configurations of the nearest C atoms change to [He] $2s^{1.298}2p^{2.840}$ and [He] $2s^{1.298}2p^{2.861}$, respectively. About 0.936e (1.445e) electrons of La-6s (Eu-6s) transfer to SWCNT, but the electrons of 5d orbital increase slightly for a contribution of back-donation of the occupied orbitals of SWCNT. Other doping cases are similar to them. So the interaction between RE atoms and SWCNT is primarily ionic due to the charge transfer from RE-6s orbital to C-2p orbital. As we know, the magnetic moments of La and Eu atoms are predominantly contributed by the polarized 5d6s electrons and the localized 4f electrons. Upon doping, most of the 6s electrons of La transfer to C-2p orbital and the 4f electrons of Eu remain in the orbital. It may be the reason why the magnetic moment of Eu is preserved but that of La is zero.

In order to observe the change in the band structures of pure tubes induced by the adsorbates, we first presented the band structure of the pure (6, 0) and (8, 0) tubes in Fig. 2. Note that the bare (6, 0) SWCNT is metallic with the top of valence bands crossing the Fermi level. For the pure (8, 0) SWCNT, the valence band maximum (VBM) and the conduction band minimum (CBM)

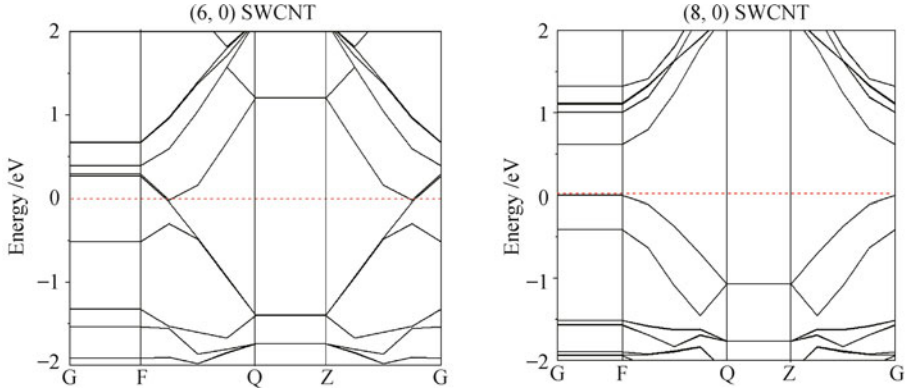

Fig. 2 Band structures of the pure (6, 0) and (8, 0) SWCNTs, respectively. The horizontal dotted line represents the Fermi energy level.

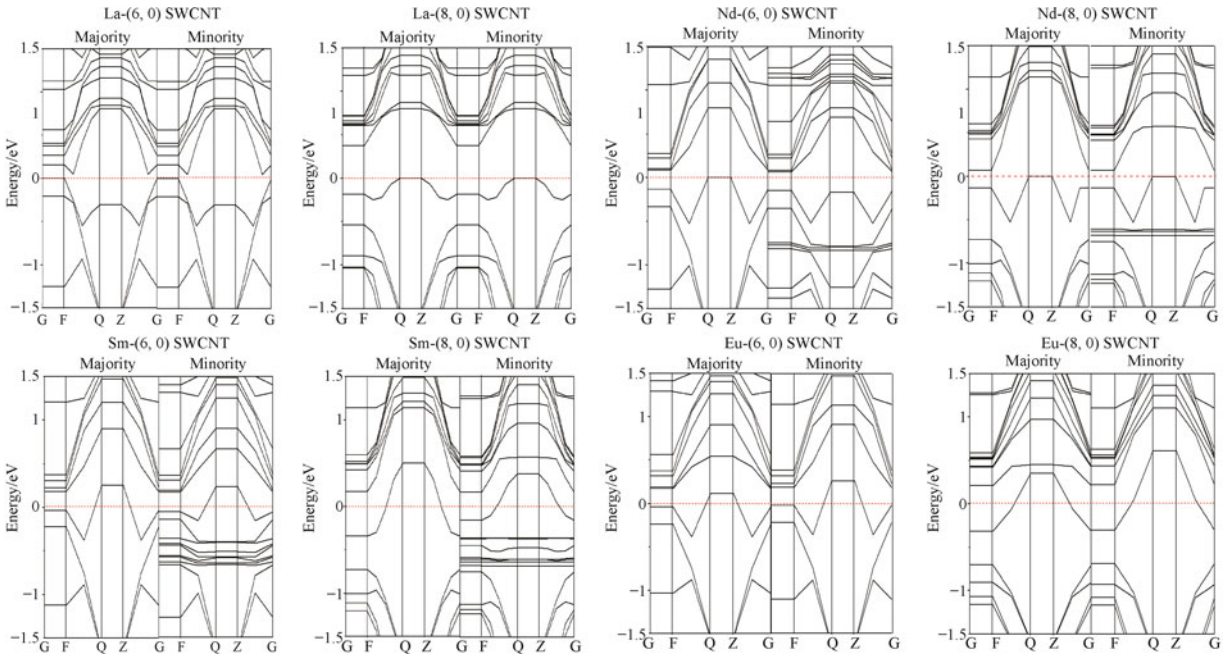

Fig. 3 Band structures for La doped (6, 0) and (8, 0) SWCNTs, Nd doped (6, 0) and (8, 0) SWCNTs, Sm doped (6, 0) and (8, 0) SWCNTs and Eu doped (6, 0) and (8, 0) SWCNTs, respectively. The horizontal dotted line represents the Fermi energy level.

are both located at F symmetry point with a gap (F–F) of 0.619eV, which is in good agreement with 0.620 eV reported in the previous literature [43]. Clearly the (8, 0) SWCNT is a direct-gap semiconductor. The spin-polarized band structures of adsorbed rear-earth atoms (La, Nd, Sm and Eu) were displayed in Fig. 3. We find that the majority (spin-up) and minority (spin-down) band structures of La doped tubes are identical with the zero magnetic moment of La atom. For La doped metallic (6, 0) SWCNT, there is an opening of a small gap (0.049 eV) just near the Fermi energy, making it close to a semimetal. Comparing the bands of La doped (8, 0) SWCNT with those of the bare (8, 0) SWCNT (in Fig. 2), we have learned that a valence band of La lies near the Fermi level and the energy gap deceases to 0.376 eV. In the case of Nd doped (6, 0) SWCNT, the majority spin state is semi-metallic with an energy gap of 0.085 eV and the minority spin state is semiconducting with a gap of 0.212 eV. Whereas a different case occurs for Nd adsorbed on (8, 0) SWCNT where both the spin-up and spin-down states are semimetal and whose energy gap is about 0.069 eV. The system of Sm doped (6, 0) SWCNT remains metallic. Meanwhile the majority bands in the vicinity of Fermi level are only slightly perturbed, but the minority bands show hybridization between Sm and (6, 0) SWCNT below the Fermi level, which also takes place in Nd and Eu situations. By the latter analysis of PDOS, It is found that the hybridization is contributed by RE-4f and C-2p states. After Sm is adsorbed on the semiconducting (8, 0) tube, a band of dopant atom crosses the Fermi level and both the majority and minority states become conductors. Similar behavior can be obtained for the systems of Eu doped (6, 0) and (8, 0) nanotubes. These results mean that the conducting properties of nanotubes can be modified by doping RE atoms.

To evaluate more on electronic structure and the spin-up and spin-down states, we presented the total density of states (TDOS) and the projected density of states (PDOS) of all the configurations. For the band structures, we first calculated the TDOS of the pristine (6, 0) and (8, 0) SWCNTs. The TDOS and PDOS after having doped RE atoms (La, Nd, Sm and Eu) were shown in Fig. 4 through Fig. 7. We first analyzed the DOS of RE doped semiconducting (8, 0) SWCNT. In Fig. 4, the majority and minority PDOS of La atom are asymmetric. The overlap of density states between La-5d, 6s and C-2p orbitals appears in the range from −0.544 eV to 2.449 eV near the Fermi level, where the hybridization takes place. This agrees with the mulliken analysis that some electrons transfer between La-5d, 6s and C-2p orbitals. In the case of Eu (in Fig. 7), the TDOS picture changes slightly compared with that of the pure (8, 0) tube, and the majority and minority PDOS are not asymmetric. There are also hybridizations of atomic orbitals between Eu-5d, 6s and C-2p orbitals (−0.541 eV to 3.537 eV) and between Eu-5p and C-2s (−23.130 eV to 18.096 eV), which is similar to the electronic structure of Eu doped C_{60}. The filled spin-up PDOS of Eu-4f orbital is much localized with a sharp peak at −0.952 eV, but the empty spin-down PDOS is very small at about 3.047 eV. It confirms that the positive spin magnetic moment of Eu is

mostly contributed by the spin-up 4f state. For the cases of other RE atoms (Nd and Sm) doped (8, 0) tube, the density of states are similar with Eu doped (8, 0) tube in some aspects, but there are some differences among them. For the PDOS of Nd (in Fig. 5), a spin-up peak and a spin-down peak of Nd-4f state are found around 0.095 eV and 2.517 eV, respectively. Due to the contribution of the Nd-4f state, the TDOS (0 eV to 3.401 eV) is more localized than those of other doping. Opposite to Eu doped (8, 0) SWCNT, the filled minority peak of Sm-4f state appears at −0.571 eV and the empty majority peak is small at 3.050 eV (in Fig. 6). So the magnetic moment of Sm is negative (in Table 1), which can also be observed in the Nd case. For (6, 0) tube, we want to explore whether the metallic nature of the tube can influence the electronic structure in any essential manner. However, it is found that the overall behavior of DOS appears to be similar for the adsorption of RE on both the (8, 0) and (6, 0) tubes. The TDOS plot of the (6, 0) tube changes slightly by doping RE atoms. Hybridizations take place between RE-5d, 6s and C-2p orbitals and between RE-4f and C-2p orbitals near the Fermi level.

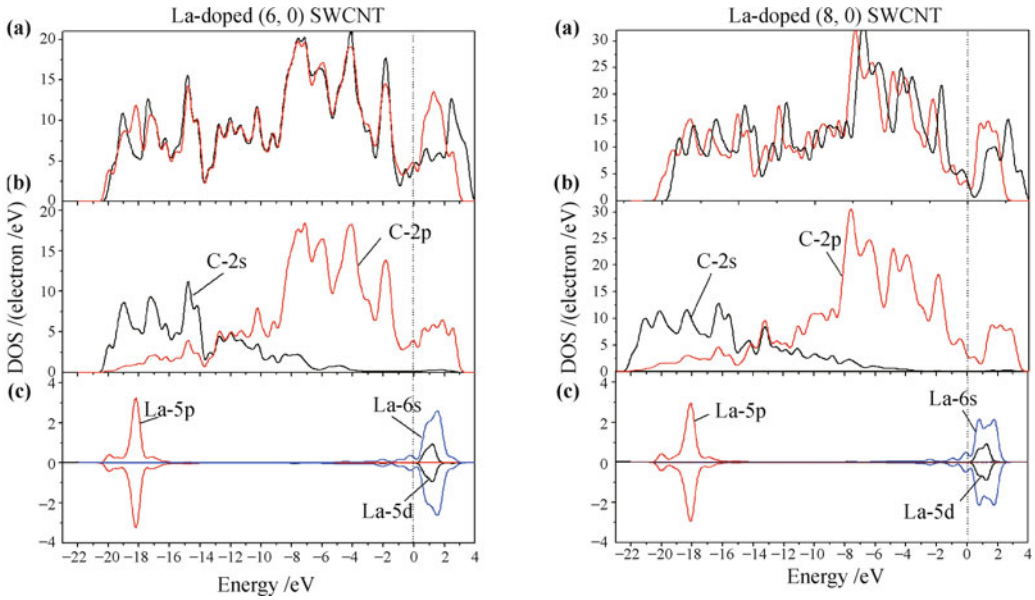

Fig. 4 The left part is the DOS of La doped (6, 0) SWCNT and the right part is the DOS of La doped (8, 0) SWCNT. **(a)** TDOS of pure SWCNT (*black line*) and La doped SWCNT (*red line*). **(b)** PDOS of C-2s orbital (*black line*) and C-2p orbital (*red line*). **(c)** PDOS of La-5p orbital (*red line*), La-6s orbital (*blue line*) and La-5d orbital (*black line*). The Fermi level is shown by the vertical dotted line.

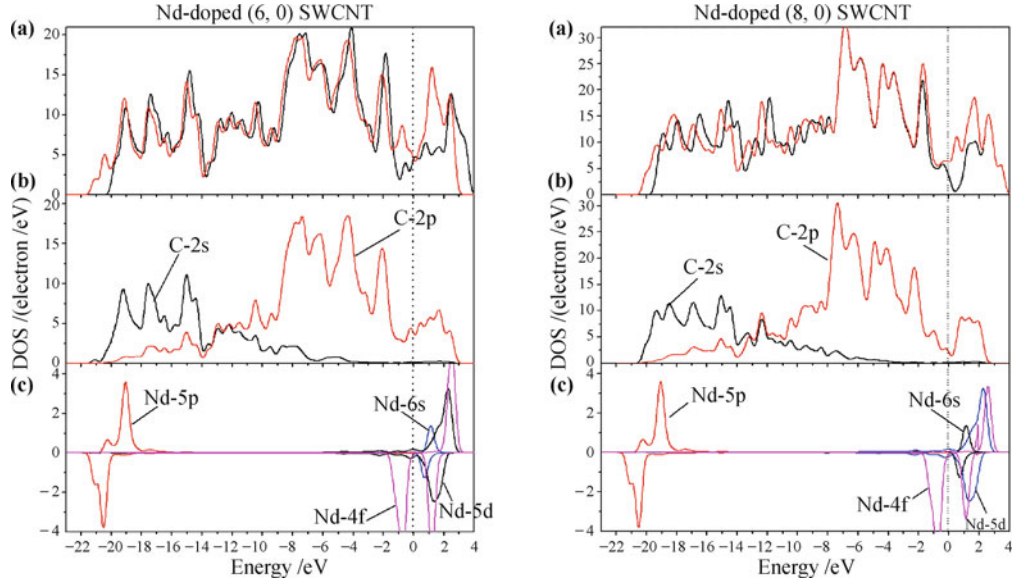

Fig. 5 The left part is the DOS of Nd doped (6, 0) SWCNT and the right part is the DOS of Nd doped (8, 0) SWCNT. **(a)** TDOS of pure SWCNT (*black line*) and Nd doped SWCNT (*red line*). **(b)** PDOS of C-2s orbital (*black line*) and C-2p orbital (*red line*). **(c)** PDOS of Nd-5p orbital (*red line*), Nd-6s orbital (*blue line*), Nd-5d orbital (*black line*) and Nd-4f orbital (*magenta line*). The Fermi level is shown by the vertical dotted line.

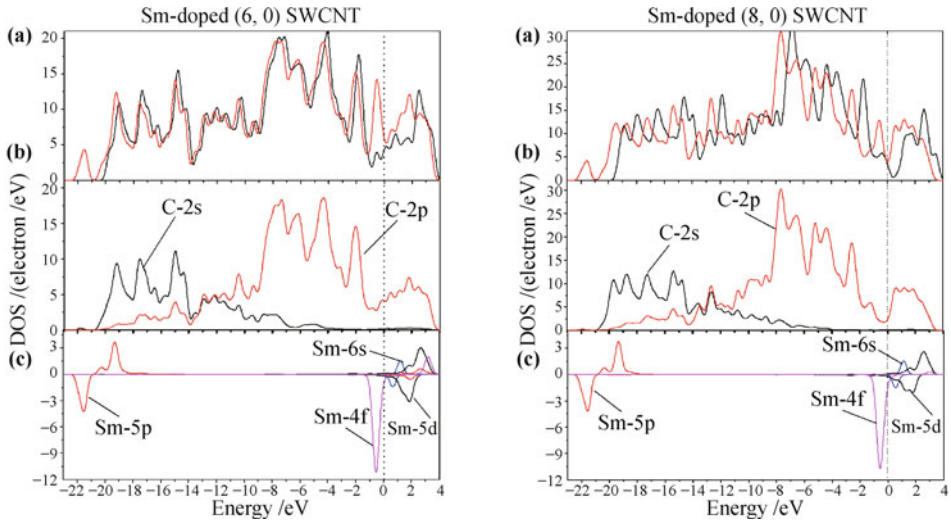

Fig. 6 The left part is the DOS of Sm doped (6, 0) SWCNT and the right part is the DOS of Sm doped (8, 0) SWCNT. **(a)** TDOS of pure SWCNT (*black line*) and Sm doped SWCNT (*red line*). **(b)** PDOS of C-2s orbital (*black line*) and C-2p orbital (*red line*). **(c)** PDOS of Sm-5p orbital (*red line*), Sm-6s orbital (*blue line*), Sm-5d orbital (*black line*) and Sm-4f orbital (*magenta line*). The Fermi level is shown by the vertical dotted line.

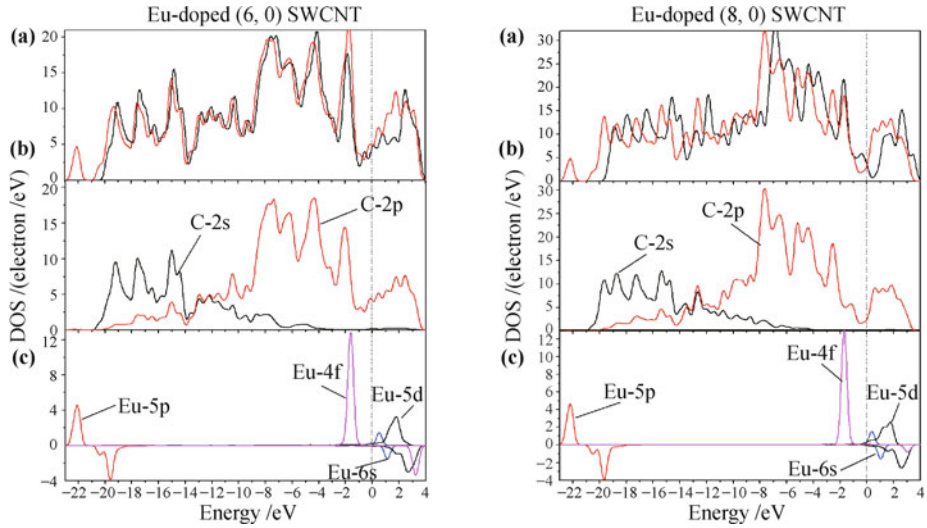

Fig. 7 The left part is the DOS of Eu doped (6, 0) SWCNT and the right part is the DOS of Eu doped (8, 0) SWCNT. **(a)** TDOS of pure SWCNT (*black line*) and Eu doped SWCNT (*red line*). **(b)** PDOS of C-2s orbital (*black line*) and C-2p orbital (*red line*). **(c)** PDOS of Eu-5p orbital (*red line*), Eu-6s orbital (*blue line*), Eu-5d orbital (*black line*) and Eu-4f orbital (*magenta line*). The Fermi level is shown by the vertical dotted line.

4 Conclusions

In summary, the ab initio method at the density functional theory (DFT) has been performed to study the interaction between RE atoms (La, Nd, Sm and Eu) and SWCNTs ((6, 0) and (8, 0)). It was found that trends in the adsorptions of RE atoms on the (6, 0) and (8, 0) tubes are similar except that the values of binding energy in the former are consistently lower. This behavior was attributed to the relatively bigger curvature of the (6, 0) tube. By Mulliken analysis, we learned that the charge transfer basically occurs between RE-5d, 6s and C-2p orbitals. SWCNTs are predicted to behave as electronic donors and the RE atoms serve as acceptors. Magnetic moments of RE atoms (Nd, Sm and Eu) are preserved after doping. The band structures and TDOS of the pristine SWCNTs are affected slightly and the electrical conductivity is changed by the doping. The study of the electronic structure and the Mulliken analysis highlight that the RE atoms and CNTs interact strongly and hybridizations take place between RE-5d, 6s and C-2p orbitals and between RE-4f and C-2p orbitals. These results may be helpful to understand the influence of RE metals on carbon tubes, and these systems could assist magnetic devices and spintronics applications. We hope this study will attract further study in the properties of RE atoms doped CNTs.

Acknowledgements H. Zhang acknowledges the financial sup-

port from the National Natural Science Foundation of China (NSFC. Grant No. 11074176 and NSAF. Grant No. 10976019) and the support from the Research Fund for the Doctoral Program of Higher Education of China (Grant No. 20100181110080).

References

1. S. Iijima, Nature, 1991, 354(7): 56
2. M. S. Dresselhaus, G. Presselhaus, and P. Avouris, Carbon Nanotubes: Synthesis, Structure, Properties, and Applications, Heidelberg: Springer, 2001
3. Z. X. Guo and X. G. Gong, Front. Phys. China, 2009, 4(3): 389
4. P. L. McEuen, M. S. Fuhrer, and H. Park, IEEE Trans. Nanotech., 2002, 1 (1): 78
5. Y. C. Sui, R. Skomski, K. D. Sorge, and D. J. Sellmyer, Appl. Phys. Lett., 2004, 84(9): 1525
6. T. Yildirim and S. Ciraci, Phys. Rev. Lett., 2005, 94(17): 175501
7. W. Z. Lia, C. H. Liang, J. S. Qiu, W. J. Zhou, H. M. Han, Z. B. Wei, G. Q. Sun, and Q. Xin, Carbon, 2002, 40(5): 791
8. Y. Yagi, T. M. Briere, M. H. F. Sluiter, V. Kumar, A. A. Farajian, and Y. Kawazoe, Phys. Rev. B, 2004, 69(7): 075414
9. F. Li, J. J. Zhao, and L. X. Sun, Front. Phys., 2011, 6(2): 214
10. M. Li, Y. F. Li, Z. Zhou, and P. W. Shen, Front. Phys., 2011, 6(2): 224
11. H. Zhang and X. D. Li, Front. Phys., 2011, 6(2): 231
12. X. Zhou, J. Zhou, K. Lü, and Q. Sun, Front. Phys., 2011, 6(2): 220
13. J. H. Lan, D. P. Cao, and W. C. Wang, J. Phys. Chem. C, 2010, 114(7): 3108
14. Z. J. Shi, Y. F. Lian, X. H. Zhou, Z. N. Gu, Y. G. Zhang, S. Iijima, L. X. Zhou, K. T. Yue, and S. L. Zhang, Carbon, 1999, 37(9): 1449
15. A. Thess, R. Lee, P. Nikolaev, H. J. Dai, P. Petit, J. Robert, C. Xu, Y. H. Lee, S. G. Kim, A. G. Rinzler, D. T. Colbert, G. E. Scuseria, D. Tomanek, J. E. Fischer, and R. E. Smalley, Science, 1996, 273(5274): 483
16. H. J. Jeong, K. H. An, S. C. Lim, M. S. Park, J. S. Chang, and Y. H. Lee, Chem. Phys. Lett., 2003, 380(3): 263
17. C. Jo, C. Kim, and Y. H. Lee, Phys. Rev. B, 2002, 65(3): 035420
18. J. J. Zhao, A. Buldum, J. Han, and J. P. Lu, Phys. Rev. Lett., 2000, 85(8): 1706
19. J. W. Zheng, S. M. L. Nai, M. F. Ng, P. Wu, J. Wei, and M. Gupta, J. Phys. Chem. C, 2009, 113(3): 14015
20. E. Durgun, S. Dag, V. M. K. Bagci, O. Gülseren, T. Yildirim, and S. Ciraci, Phys. Rev. B, 2003, 67(20): 201401
21. E. Durgun, S. Dag, S. Ciraci, and O. Gülseren, J. Phys. Chem. B, 2004, 108(2): 575
22. Y. L. Mao, X. H. Yan, and Y. Xiao, Nanotechnology, 2005, 16(12): 3092
23. A. Vdomveoh, T. Kerecharoen, and T. Osotchan, Chem. Phys. Lett., 2005, 406(2): 161
24. Y. J. Kang, J. Choi, C. Y. Moon, and K. J. Chang, Phys. Rev. B, 2005, 71(11): 115411
25. V. V. Ivanovskaya, C. Köhler, and G. Seifert, Phys. Rev. B, 2007, 75(7): 075410
26. X. X. Wang, X. H. Yan, and Y. Xiao, Nanotechnology, 2005, 16(12): 3092
27. J. C. Xie, Y. J. Tang, and H. Zhang, Cent. Eur. J. Phys., 2010, 9(3): 716
28. Z. W. Zhang, J. C. Li, and Q. Jiang, J. Phys. Chem. C, 2010, 114(8): 7733
29. J. P. Perdew and Y. Wang, Phys. Rev. B, 1992, 45(23): 13244
30. B. Delley, J. Chem. Phys., 2000, 113(18): 7756
31. Y. Luo, J. Baldamus, O. Tardif, and Z. Hou, Organometallics, 2005, 24(18): 4362
32. C. M. Fang, J. Bauer, J. Y. Saillard, and J. F. Halet, J. Solid State Chem., 2007, 180(9): 2465
33. A. Delin, P. M. Oppeneer, M. S. S. Brooks, T. Kraft, J. M. Wills, B. Johansson, and O. Eriksson, Phys. Rev. B, 1997, 55(16): R10173
34. S. J. S. Jalali Asadabadi and H. Akbarzadeh, Physica B, 2004, 76(4): 349
35. A. Rubio-Ponce, A. Conde-Gallardo, and D. Olguín, Phys. Rev. B, 2008, 78(13): 035107
36. A. Delin, L. Fast, B. Johansson, O. Eriksson, and J. M. Wills, Phys. Rev. B, 1998, 58(8): 4345
37. B. Delley, Phys. Rev. B, 2002, 66(15): 155125
38. H. J. Monkhorst and J. D. Pack, Phys. Rev. B, 1976, 13(12): 5188
39. O. Gülseren, T. Yildirim, and S. Ciraci, Phys. Rev. Lett., 2001, 87(11): 116802
40. H. Kuramochi, T. Vzumaki, M. Yamka, H. Akinaga, and H. Yokoyama, Nanotechnology, 2005, 16(1): 24
41. L. Zhu, K. L. Yao, and Z. L. Liu, Solid State Commun., 2007, 141(11): 628
42. G. L. Lu, K. M. Deng, H. P. Wu, J. L. Yang, and X. Wang, J. Chem. Phys., 2006, 124(5): 054305
43. X. Blasé, L. X. Benedict, E. L. Shirley, and S. G. Louie, Phys. Rev. Lett., 1994, 72(12): 1878